Endocrine, *vol. 23, nos. 2–3, 199–213, March–April 2004* 0969–711X/04/23:199–213/$25.00

Stepwise Posttranslational Processing of Progrowth Hormone-Releasing Hormone (proGHRH) Polypeptide by Furin and PC1

Samuel F. Posner,[1] Charles A. Vaslet,[1] Michelle Jurofcik,[1] Alisson Lee,[1] Nabil G. Seidah,[2] and Eduardo A. Nillni[1]

[1]Division of Endocrinology, Department of Medicine, Brown Medical School, Rhode Island Hospital, Providence, Rhode Island 02903; and [2]Laboratory of Biochemical Neuroendocrinology, Clinical Research Institute of Montreal, Montreal, Quebec H2W1R7, Canada

Through a posttranslational processing mechanism, progrowth hormone releasing hormone (proGHRH) gives rise to an amidated GHRH molecule, which in turn stimulates the synthesis and release of growth hormone. We have previously proposed a model for the biochemical processing of proGHRH [Nillni et al. (1999), *Endocrinology* 140, 5817–5827]. We demonstrated that the proGHRH peptide (10.5 kDa, 104 aa) is first processed to an 8.8 kDa intermediate form that is later cleaved to yield two products: the 5.2 kDa GHRH and the 3.6 kDa GHRH-RP. However, the proteolytic enzymes involved in this process are unknown. Therefore, in this study we determined which proconverting enzymes are involved in this process. We transfected different constructs in cell lines carrying different PC enzymes followed by analysis of the peptide products after metabolic labeling or Western blots. We found that in the absence of furin (LoVo cells) or CHO cells treated with BFA, only one moiety was observed, and that corresponds to the same electrophorectic mobility to the GHRH precursor. This finding strongly supports an initial role for furin in the processing of proGHRH. The results from transfections with preproGHRH alone or double or triple transfections with PC1 and PC2 in AtT-20, GH3, and GH4C1 cells indicated that PC1 is the primary enzyme involved in the generation of GHRH peptide from the 8.8 kDa intermediate form. We found that AtT-20 cells (high PC1, very low PC2) were able to generate GHRH. However, GH3 cells (high PC2, but not PC1) were able to process the 8.8 kDa peptide to GHRH only after the cotransfection with the PC1 enzyme. Transfections with preproGHRH-GFP and preproGHRH-V5 provided similar results in all the cell lines analyzed. These data support the hypothesis that proGHRH is initially cleave by furin at preproGHRH29-30, followed by a second cleavage at preproGHRH74 primarily by PC1 to generate GHRH and GHRH-RP peptides, respectively.

Key Words: proGHRH; GHRH; prohormone; processing; convertases; PC1; PC2; furin; peptide sorting.

Introduction

Peptide hormones are often initially synthesized as inactive prohormone precursors, which are then appropriately cleaved into active molecules *(1,2)*. In the neuroendocrine and endocrine systems, this extensive activation process involves the regulated secretory pathway. The regulated secretory pathway consists of the rough endoplasmic reticulum (RER), the Golgi apparatus, and the secretory granules (SGs) *(3)*. These organelles house the enzymes necessary for the appropriate posttranslational modifications that alter the structure of the prohormone and convert it into its mature and active form(s) *(1,2)*. Growth hormone-releasing hormone (GHRH) is one such peptide hormone that participates in the aforementioned pathway *(4)*. Its precursor, progrowth hormone-releasing hormone (proGHRH), similarly to other neuropeptide precursors in the hypothalamus, is believed to be cleaved by members of the subtilisin-like group of proprotein convertases (PCs) *(4)*. Seven members of this family have been identified in mammals: furin, PC2, PC3/PC1, PC4, PACE4, PC5/PC6, and PC7/PC8/LPC *(1,2)*. Analysis of tissue distribution demonstrates a unique pattern for each of the seven enzymes that comprise this family. PC1/PC3, PC2, and PC5 are the only members that are found solely in endocrine and neuroendocrine tissues and cells with similar substrate specificity to PC1 *(5)*. The enzyme furin, on the other hand, is ubiquitously present in all cells. This, in addition to other studies, suggests that PC1/PC3 and PC2 are the major processing enzymes of the prohormones destined to the regulated secretory pathway. These enzymes are calcium-dependent serine endoproteases

Received January 12, 2004; Revised March 1, 2004; Accepted March 5, 2004.

Author to whom all correspondence and reprint requests should be addressed: Dr. Eduardo A. Nillni, Division of Endocrinology, Rhode Island Hospital, 55 Claverick Street, Fourth Floor, Room 430, Providence, RI 02903. E-mail: Eduardo_Nillni@Brown.edu

and are related to the subtilisin and the yeast processing protease, kexin. The importance of understanding the posttranslational modifications of proGHRH lies in the ability of its mature form, GHRH, to increase the secretion and synthesis of growth hormone (GH), a hormone whose main function is to regulate overall body growth, but which also plays an important role in intermediary metabolism *(6–8)*.

Rat preproGHRH (104 amino acids [aa]) consists of a characteristic 19 aa signal peptide, the 44 aa GHRH, and the 31 aa GHRH-RP C terminal peptide *(4)*. Correct trafficking and sorting of preproGHRH is imperative for the proper function of its products. After the signal peptide targets the translating preproGHRH to the RER, it is cleaved off, producing proGHRH. The prohormone is then imported to the lumen of the ER, transported to the Golgi apparatus, and then sorted into SGs where it will be stored until the cell is stimulated causing the granules to release their content through exocytosis. During this seemingly straightforward process, the targeting and sorting of the molecules to the correct SGs is key. Specifically, the SGs play many essential roles: they can provide for the acute export of secretory proteins in excess of biosynthetic capacity, they can enable quantal secretion of bioactive peptides that are regulated not only by intensity but also by frequency of stimulation, and most relevant to the current topic, they can provide a compartment for sustained proteolytic processing and other posttranslational modifications required for the synthesis of peptide hormones. Posttranslational modifications include glycosylation, phosphorylation, protein folding, and endoproteolytic cleavage *(9,10)*. Enzymes that are housed in the SGs recognize the molecule as it enters and then make the necessary modifications.

The processing of proGHRH has been shown to produce several peptide moieties. We previously radiolabeled and immunoprecipitated the cell content and release media of primary cultures of hypothalamic neurons, an endogenous source of proGHRH, PC1, and PC2. The peptides were immunoprecipitated with antibodies against the GHRH and GHRH-RP. Using pulse-chase analysis, we demonstrated that the signal peptide of the 12.3 kDa preproGHRH$_{1–104}$ was first cleaved to produce a 10.5 kDa proGHRH (preproGHRH$_{20–104}$) molecule. Subsequent cleavage produced an 8.8 kDa preproGHRH$_{31–104}$, which included both GHRH and GHRH-RP molecules. A single cleavage separated GHRH and GHRH-RP to form a 5.2 kDa preproGHRH$_{31–73}$ (GHRH) and a 3.6 kDa preproGHRH$_{74–104}$ (GHRH-RP). GHRH was cleaved once more to produce 1.5 kDa and 3.5 kDa fragments. The molecular weight estimates obtained by SDS-PAGE suggests possible cleavage sites at monobasic residues or pairs of basic residues, consistent with cleavage by prohormone convertases. This proposed model of processing is shown in Fig. 1 *(4)*.

Evidence both for and against the processing of proGHRH in the regulated SGs led to a study in our laboratory, which

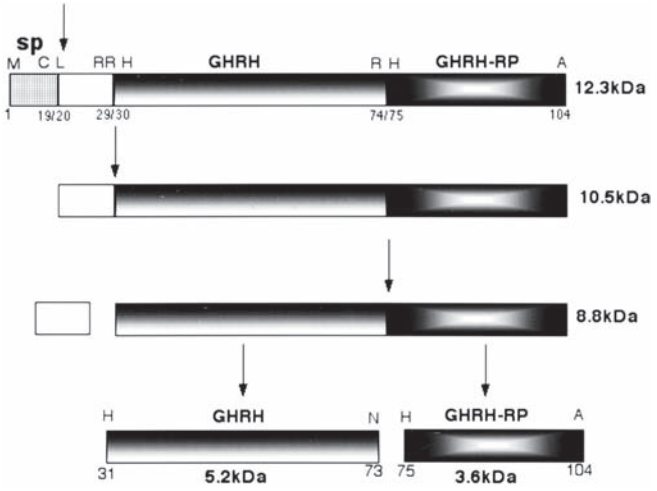

Fig. 1. Proposed model of proGHRH processing to its end products as previously described by us [Nillni et al. (1999). *Endocrinology* **140,** 5817–5827]).

treated cells with either PMA as a secretagogue or regular medium. Cultures treated with PMA released considerably more GHRH into the release medium than unstimulated cells. This supported the hypothesis that GHRH is processed and released by the regulated secretory pathway. However, material released under unstimulated conditions may represent a previously defined constitutive-like secretion of the hormone *(3)*.

The selective expression of PC1 and PC2 in endocrine and neuroendocrine cells specifically suggests they may be significant in prohormone processing *(5,11–14)*. PC1 and PC2 have been shown to process proTRH *(15–18)*, proinsulin *(19–21)*, proenkephalin *(22)*, prosomatostatin *(22)*, and POMC *(23,24)* to various intermediates and end products in coexpression experiments. The fact that PC1, PC2, and PC5 are endogenous constituents in rat hypothalamic neuronal cells suggests that these endopeptidases could be involved in proGHRH processing. Therefore, we speculated that similarly to other neuropeptides, the processing of proGHRH was probably dependent on PC1, PC2, or furin enzymatic activity. To this purpose, we have generated different preproGHRH cDNA contructs fused with the green fluorescence protein (GFP), Flag epitope at the N-terminal side, and V5 epitope at the C-terminal side of proGHRH, as well as wild-type preproGHRH. These unique constructs were transfected into different cell lines containing endogenous PC1 or PC2 and furin or lacking some or all of them. PC1 and/or PC2 cDNA were cotransfected with the preproGHRH cDNA. We also determined that the routing of proGHRH fused to a big tag such as GFP did not prevent its targeting to the regulated secretory pathway in tumoral cell lines. The colocalization of proGHRH with PC1 in hypothalamic neuronal cells was also determined. Taken together, in this study

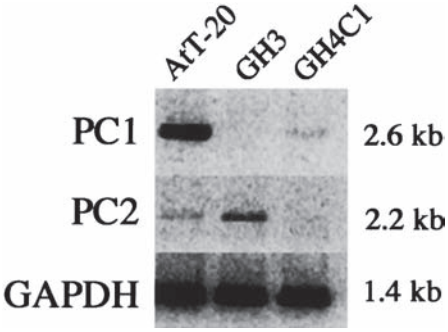

Fig. 2. RT-PCR results for PC1 and PC2 transcriptional activity in AtT-20, GH3, and GH4C1 cells. Total RNAs from AtT-20, GH3 and GH4C1 cells were subjected to RT-PCR using sequence-specific amplification primers (Materials and Methods). The upper panel shows PC1 results and the middle panel PC2 results. The lower panel shows levels of GAPDH product in the same samples.

we show the evidence of a stepwise processing of proGHRH implicating primarily furin and PC1.

Results

PC1 is the Primary Enzyme Involved in the Generation of GHRH and GHRH-RP

Radiolabeling Studies

In an effort to determine which PC enzyme may be involved in the generation of GHRH peptide, we transiently transfected three different cell lines carrying different levels of PC enzymes with preproGHRH cDNA and/or cotransfected with PC2 or PC1 cDNAs. As a source of PC1 we used AtT-20 cells, a well-defined mouse corticotropic cell line that contains high levels of PC1 and also expresses low levels of PC2, in addition to furin, PC5, PC7, and PACE. The GH3 cells, a growth hormone cell line with similar morphology to epithelial cells, produces growth hormone and prolactin. GH3 has been shown to contain endogenous PC2 and no PC1 *(5,12)* and the GH4C1 cell line, a variation of the GH3 cell line that produces prolactin and very low levels of growth hormone. GH4C1 contains neither PC1 nor PC2 *(5)*. Because frequent cell line passages could change their genetic make up over time, we determined the transcriptional activity of PC1 and PC2 by RT-PCR. Figure 2 depicts a typical RT-PCR for the three cell lines used, where AtT-20 showed a strong presence of PC1 and a low level of PC2, GH3 cells only exhibited the presence of PC2, and GH4C1 cells showed very low levels of PC1. Even though some minor level of transcriptional activity was observed for PC1 (Fig. 2), this does not reflect in any PC1 activity as demonstrated in processing studies done for many prohormones using the GH4C1 cells *(15,22,25–27)* and in the present study.

In order to determine the effects of endogenous PC1 in addition to transfected levels of PC2, AtT-20 cells were transfected with preproGHRH or cotransfected with preproGHRH and PC2 cDNAs. These cells were then radiolabeled with [^{3}H]leucine, [^{3}H]tryptophan, and [^{3}H]valine. Untransfected cells were also radiolabeled and served as a control. Acid-extracted proGHRH-derived peptides were immunoprecipitated using two antibodies, anti-GHRH and anti-GHRH-RP, and then visualized by SDS-PAGE following peptide extraction and counting.

Immunoprecipitated peptides derived from radiolabeled AtT-20 cells revealed the presence of three major peptide peaks with an electrophoretic mobility around a 10.5, 8.8, and 5.2 kDa molecular mass (MM) (Fig. 3A). These moieties were similar in size to those previously described by our group in pulse-chase experiments using primary cultures of hypothalamic neurons *(4)* that corresponds to the proposed rat GHRH precursor (10.5 kDa, preproGHRH$_{20–104}$), the intermediate form (8.8 kDa, preproGHRH$_{31–104}$), and GHRH (5.2 kDa, preproGHRH$_{31–73}$), respectively. The 5.2 kDa peptide had the same electrophoretic mobility as the synthetic ^{125}I-GHRH. The addition of PC2 in the transfection seemed to enhance the level of GHRH and diminish the 10.5 kDa precursor (Fig. 3B). As expected, untransfected cells and release media from all experiments showed no radioactivity (not shown).

The second antibody applied was anti-GHRH-RP *(4)*. The transfection of AtT-20 cells with preproGHRH produced two distinct peaks and a third slight peak with approximate molecular masses of 10.5 kDa, 8.8 kDa, and 3.6 kDa, respectively (Fig. 3C). The addition of PC2 cDNA (Fig. 3D) did not greatly alter the 3.6 kDa peptide profile as compared with Panel C of the same figure; however, the 8.8 kDa peak was wider. Similarly to the experiments performed using anti-GHRH, no trace of radioactivity was found in either the release media or untransfected cells. Altogether, these results indicate that PC2 has some minor effect on the conversion of the 8.8 kDa form to GHRH and no effect on GHRH-RP.

The role of endogenous PC2 alone and endogenous PC2 in addition to transfected levels of PC1 was investigated by transfecting GH3 cells with preproGHRH or cotransfecting GH3 cells with preproGHRH and PC1. A control using nontransfected cells was also performed. These cells were then radiolabeled with [^{3}H]leucine, [^{3}H]tryptophan, and [^{3}H]valine and immunoprecipitated using the two antibodies described above, antiGHRH and antiGHRH-RP. Using antiGHRH the SDS-PAGE distribution profile showed the presence of two moieties (Fig. 4A) of around 10.5 kDa and 8.8 kDa MM, respectively. Strikingly, cells that were transfected with PC1 cDNA showed an almost full conversion of proGHRH to its smaller forms (Fig. 4B) and a minor shoulder at the right side of the 5.2 kDa peptide. The slices correspond to the molecular masses of 8.8 kDa, 5.2 kDa,

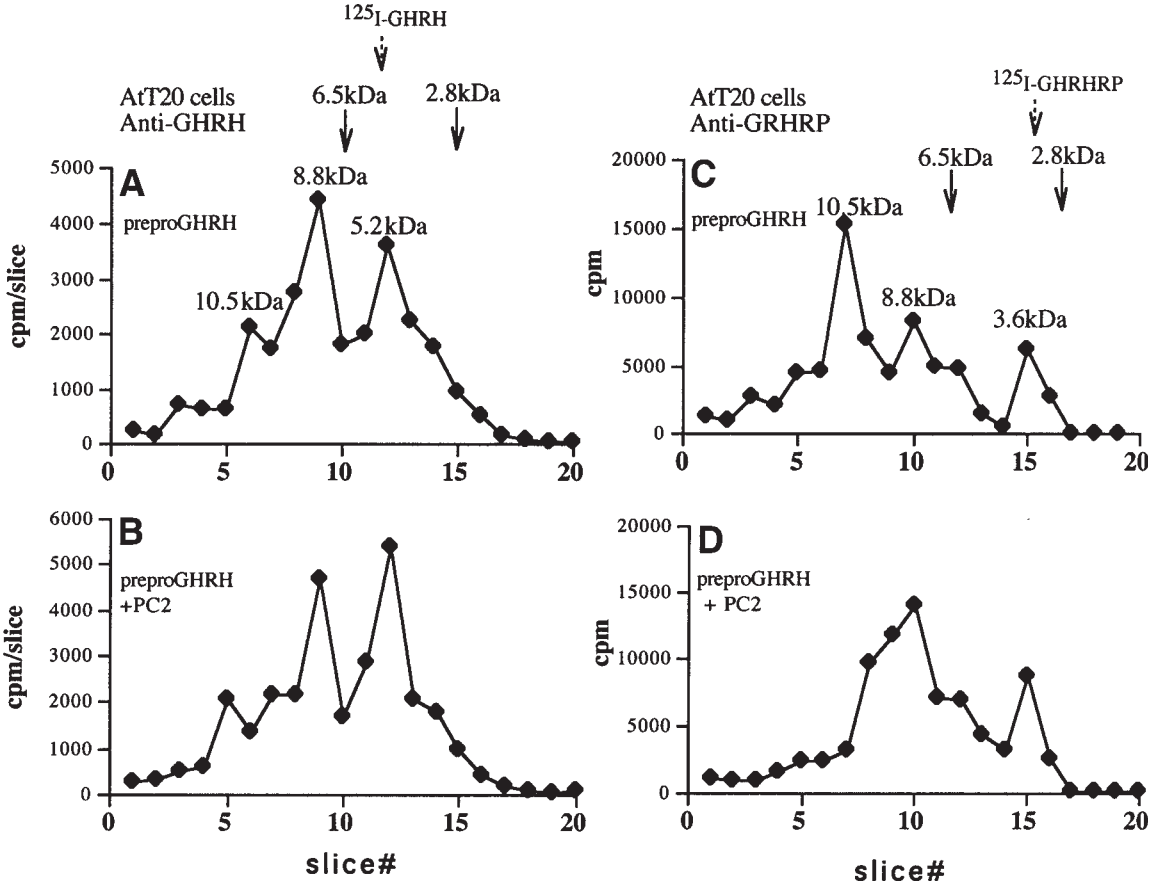

Fig. 3. Electrophoretic separation of immunoprecipitated proGHRH-derived peptides with anti-GHRH and anti-GHRH-RP in AtT-20 cells transfected with preproGHRH cDNA or cotransfected with PC2. The immunoprecipitates were electrophoresed on an SDS-polyacrylamide Tricine gel and the counts were plotted against gel slice. Molecular weights of the peaks are indicated based on the migration of molecular weight standards. This figure represents a typical profile of three independent experiments. The molecular weight markers shown in this figure are 6.5 and 2.8 kDa.

and 3.5 kDa, respectively. The release media samples and nontransfected cells were radiolabeled and immunoprecipitated with antiGHRH. The subsequent SDS-PAGE reported no traces of radioactivity (not shown).

AntiGHRH-RP was then used during the immunoprecipitation of GH3 cells transfected with either preproGHRH or preproGHRH and PC1. The profile of GH3 cells transfected with only preproGHRH showed the presence of two peaks (Fig. 4C). The molecular masses of these peptides were 10.5 kDa, and 8.8 kDa. The addition of PC1 cDNA caused the full processing of proGHRH and showed the formation of the 3.6 kDa GHRH-RP peptide (Fig. 4D). As with antiGHRH, the media and nontransfected cells showed no signs of radioactivity indicating that no peptide products were present (not shown). These data strongly suggest that PC1 is the primary enzyme involved in the formation of GHRH and GHRH-RP peptides.

We later performed the same type of studies using the regulated GH4C1 cell line because of the absence of PC1 and PC2 activity *(5,12)*. Similarly to the GH3 cells, the GH4C1 cell line contain large SGs, a prerequisite to GHRH maturation. Thus, they can be transfected in a variety of ways. The presence of one enzyme in larger quantities than the other is no longer applicable as both enzymes are expressed at a similar rate. GH4-C1 cells were transfected with preproGHRH only, preproGHRH and PC2, and finally preproGHRH, PC1, and PC2. These cells were radiolabeled with [^{3}H]leucine, [^{3}H]tryptophan, and [^{3}H]valine and immunoprecipitated using the three antibodies described above: antiGHRH, and antiGHRH-RP.

Extracts from cells transfected with preproGHRH and consequently immunoprecipitated with anti-GHRH showed the presence of two peaks with nearly identical levels of radioactivity (Fig. 5A). The peaks correlated to molecular masses of 10.5 kDa and 8.8 kDa. Transfection with preproGHRH and PC2 decreased slightly the second peak, 8.8 kDa, and a third modest peak was produced with a molecular mass around 5.2 kDa (Fig. 5B). Remarkably, when the cells were also transfected with PC1, a dramatic increase in the level of the 5.2 kDa peptide was observed (Fig. 5C). Radiolabeled peptides from GH4C1 cells were also immunoprecipitated with anti-GHRH-RP antibodies (Figs. 5D–F).

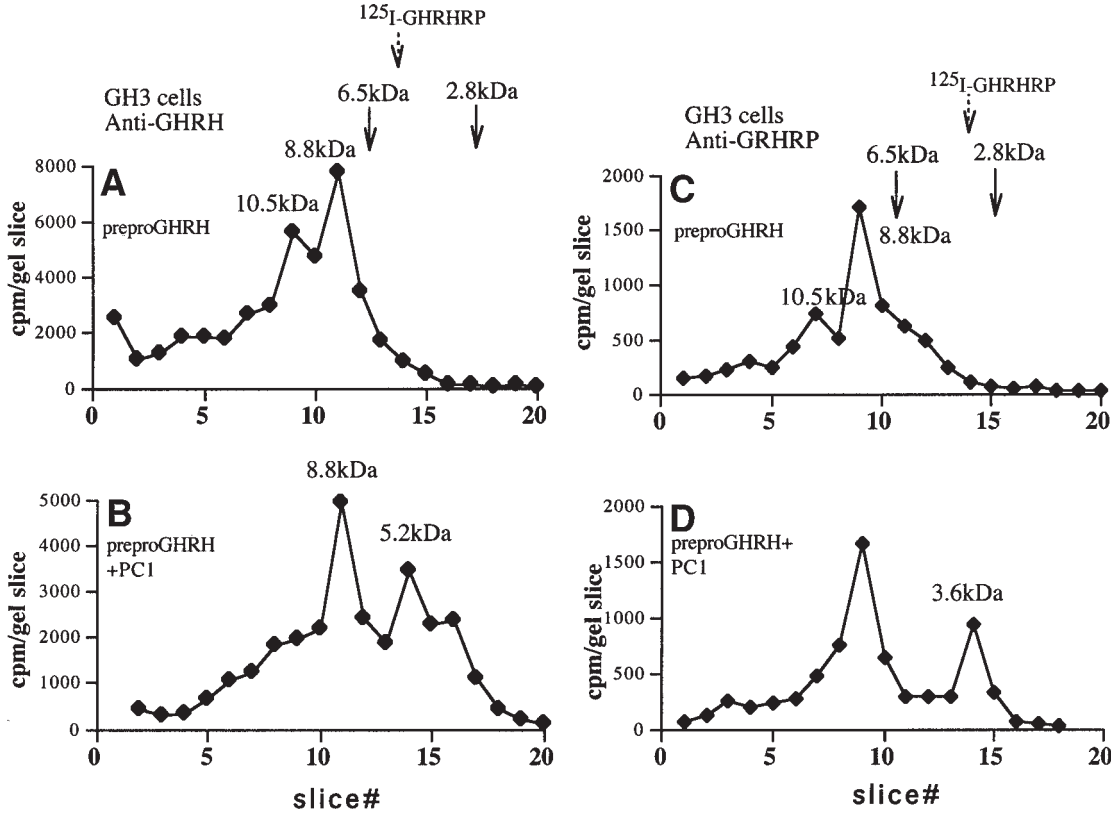

Fig. 4. Electrophoretic separation of immunoprecipitated proGHRH-derived peptides with anti-GHRH and anti-GHRH-RP in GH3 cells transfected with preproGHRH cDNA or cotransfected with PC1. The immunoprecipitates were electrophoresed on an SDS-polyacrylamide Tricine gel and the counts were plotted against gel slice. Molecular mass of the peaks are indicated based on the migration of molecular weight standards.

This antibody, when used in conjunction with GH4C1 cells transfected solely with preproGHRH, showed the presence of one distinct peptide with a molecular mass of approximately 10.5 kDa and a smaller one of around 8.8 kDa MM (Fig.5D). The addition of PC2 did not significantly change the levels of the two peptides. However, when the PC1 gene was added in the transfection, a prominent smaller peptide of about 3.6 kDa MM was formed (Fig. 5F). Taken together these results and those depicted in Figs. 3 and 4 are consistent with the hypothesis that furin present in these cells are responsible for the first cleavage of proGHRH to generate the 8.8 kDa form to be cleaved later primarily by PC1 at the preproGHRH74 to generate the GHRH and GHRH-RP peptides.

Western Blot Analysis of the Fusion Protein proGHRH-V5 and proGHRH-GFP in Three Cell Lines Containing Different Levels of PC1 and PC2

We next evaluated by Western blot analysis whether a similar profile of processing was observed when using the fusion protein proGHRH-V5 in the same cell lines described above. Peptide tags were fused to proGHRH to improve detection and reproducibility as well as to follow the processing of N- and C-terminal processed forms. Similarly to the results shown in Figs. 3–5, GH4C1, GH3, and AtT-20 cells transfected with preproGHRH-V5 were able to generate the GHRH presursor and the 8.8 kDa intermediate form attached to V5 peptide (Fig. 6A), but only AtT-20 cells that contain high levels of PC1 were able to generate the GHRH-RP peptide. We also transfected the fusion construct proGHRH-GFP and analyzed the translation products from the three cell lines in the same way. PreproGHRH-GFP cDNA was transfected into the cell lines and 2 d later the cell contents were harvested and prepared for SDS-PAGE fractionation. After fractionation, the proteins were blotted onto a membrane and probed with anti-GFP. Figure 6B shows two major bands for the three cell lines investigated when using anti-GFP antibodies. The upper band represents the entire proGHRH-GFP protein, which would be expected to have a MM of approximately 37 kDa. The lower band runs at a position that suggests it is the 8.8 kDa intermediate form fused with GFP, which would be expected to have a MM of approximately 36 kDa. Consistent with the results shown in Figs. 3–5, AtT-20 cells were able to generate a third band with the same electrophoretic mobility to the GHRH peptide. These results strongly suggest that

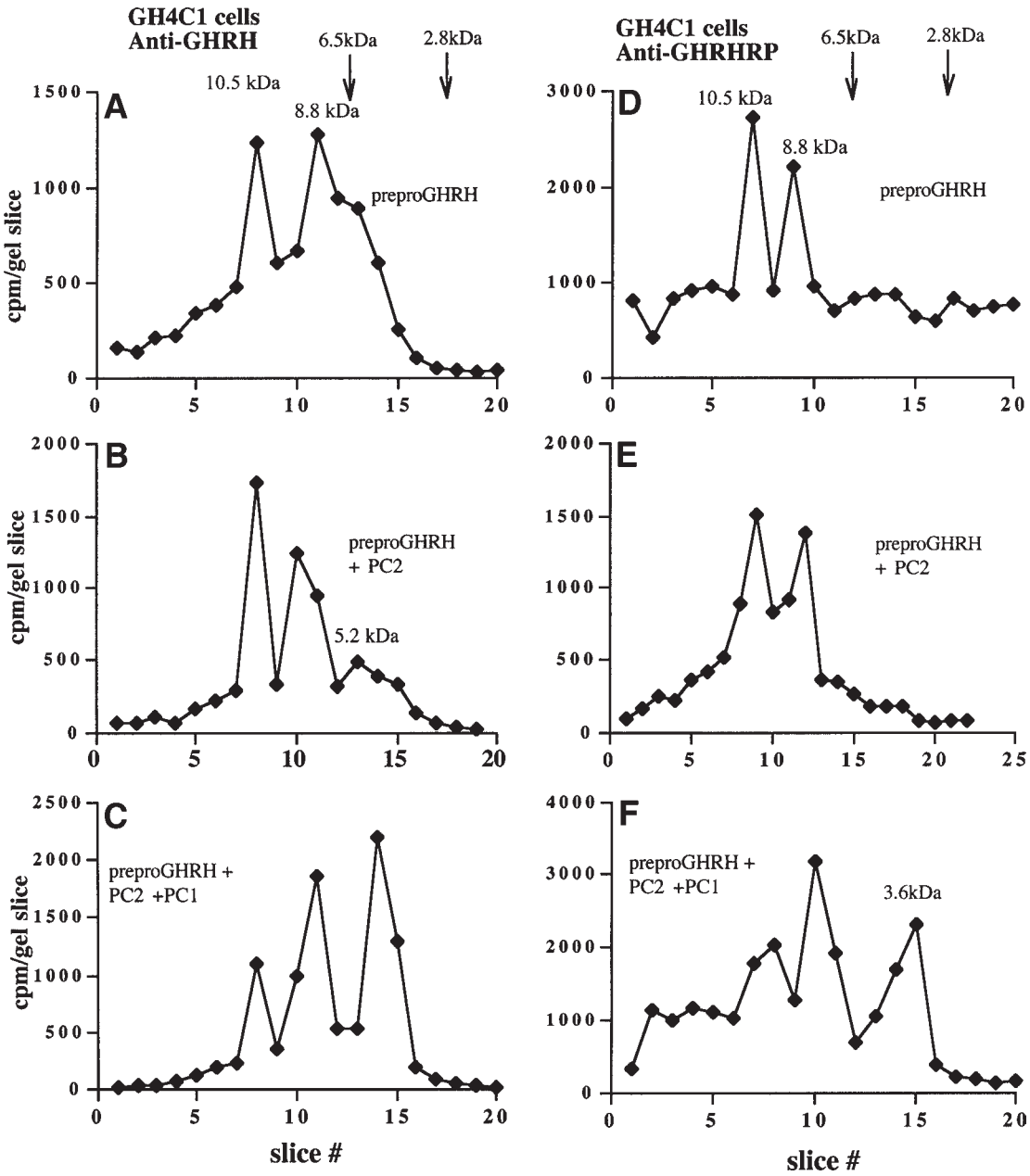

Fig. 5. Electrophoretic separation of immunoprecipitated proGHRH-derived peptides with anti-GHRH and anti-GHRH-RP in GH4C1 cells transfected with preproGHRH cDNA or cotransfected with PC1 and PC2. The immunoprecipitates were electrophoresed on an SDS-polyacrylamide Tricine gel and the counts were plotted against gel slice. Molecular mass of the peaks are indicated based on the migration of molecular weight standards. This figure represents a typical profile of three independent experiments. The molecular weight markers shown in this figure are 6.5 and 2.8 kDa.

fusion proteins proGHRH-V5 and proGHRH-GFP were correctly processed, and that the GFP tag apparently did not affect the folding and further targeting of proGHRH to the regulated secretory pathway (RSP, see below). As depicted in Fig. 6B, GH4C1 and GH3 cells were able to generate the GHRH precursor and the 8.8 kDa intermediate form, but only AtT-20 cells produced high levels of GHRH. GH3 cells showed some weak band in the area of GHRH. Again, these results further support the hypothesis that PC1 is the major enzyme involved in the processing of the 8.8 kDa intermediate giving rise to GHRH and GHRH-RP peptides by cleaving at preproGHRH$_{74}$.

ProGHRH-GFP Is Routed to the Regulated Secretory Pathway

Since GFP is a larger molecule than proGHRH itself, we wanted to determine whether the processing products shown in Fig. 6B indeed derive from processing of proGHRH within

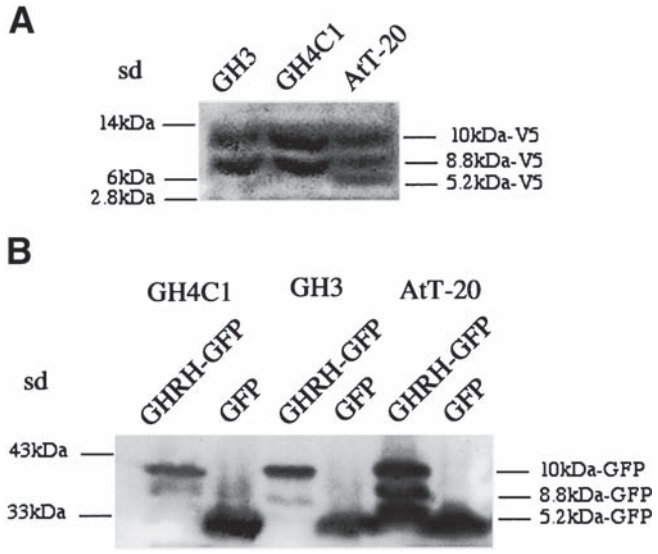

Fig. 6. Processing of the proGHRH-V5 and preproGHRH-GFP fusion proteins in three in cell lines containing different levels of PC1 and PC2. The extracted biosynthetic products from transfected cells with the proGHRH-V5 and proGHRH-GFP fusion proteins were subjected to Western blot analysis using anti-V5 and anti-GFP antibodies (V5, approx 1.5 kDa; GFP, approx 27 kDa).

the subcellular compartments of the RSP. Therefore, we transfected preproGHRH-GFP plasmid in AtT-20 cells. As depicted in Fig. 7B the processing products derived from fusion protein proGHRH-GFP were distributed along the RSP as judge by the punctual distribution in SGs located in the cell body and processes. A very similar staining pattern was shown in cells transfected with preproGHRH cDNA and visualized with anti-GHRH (Fig. 7C), whereas transfection with GFP cDNA alone showed a diffuse cytoplasmic staining. The combined results from Figs. 6 and 7 demonstrate that the translation product of the fusion protein proGHRH-GFP in these secretory and neuronal cell lines was correctly processed and sorted to the RSP similarly to the wild-type proGHRH polypeptide.

The Enzyme Furin Processes GHRH Precursor at the Amino Terminal preproGHRH29-30 Cleavage Site

We have previously proposed that the 8.8 kDa form detected in the first stages of processing is derived from an N-terminal initial cleavage at the Arg^{29}-Arg^{30} of the original preproGHRH precursor *(4)*. In this section of the study we constructed a fusion protein with the Flag tag at the amino terminal side of proGHRH specifically located between the signal peptide and proGHRH. This construct was used to transfect all the secretory cell lines used in this study including AtT-20, GH3, and GH4C1, and the extracted products were visualized by Western blot analysis using an antibody against the peptide Flag. As expected from our original hypothesis *(4)* no band was detected in any of the cell lines (not shown). Assuming that a proteolytic cleavage by furin occurs at the preproGHRH29-30 bond, this will generate a small peptide of about 1.9 kDa MM which is composed of the Flag epitope (approx 0.8 kDa) fused to a 1.1 kDa peptide. This type of peptide size is generally very difficult to detect by Western Blot analysis. However, a possibility exists that after this initial cleavage, this peptide was degraded or released in a constitutive fashion, but no band was detected in the release media of these transfections. The first time we were able to detect Flag-proGHRH polypeptide was when we used the CHO constitutive cell line (containing furin, but no PC1 or PC2) transfected with preFlag-proGHRH cDNA and subjected to brefeldin A (BFA) treatment *(28)*. Figure 8A depicts one band similar in molecular size to proGHRH plus Flag when BFA was applied for 2 h to the culture, and no band was detected in the media. Without BFA no band was observed in the cell content and the released media. This indicates that the GHRH precursor was processed and is out of detection by the anti-Flag antibody. BFA is a fungal toxin that disassembles the Golgi membranes and pushes proteins like turin back to the endoplasmic reticulum making them inactive. Using the same constitutive cell line, we transfected the preproGHRH-V5 cDNA construct and analyzed its products by Western blot. After BFA treatment one strong band similar in size to the GHRH precursor attached to V5 was observed plus a weaker band similar in mobility to the 8.8 kDa form, whereas without BFA treatment almost no bands were detected in the cell content, but were recovered in the release media (Fig. 8B). It is interesting to point out that even in the presence of BFA, some 8.8 kDa peptide was formed. These results indicate that Golgi is the site of the first proGHRH cleavage, as BFA treatment seems to disable this processing step.

The first conclusive evidence for the role of furin, which is commonly localized in the Golgi, in the processing of proGHRH at the N-terminal side of the prohormone came from the results presented in Fig. 8C where LoVo cells lacking furin were transfected with preproGHRH-GFP cDNA. We elected to use the proGHRH-GFP fusion protein in most of these experiments because it provided us with more reproducible results in terms of the ability of the GFP antibody to recognize bands with very little material. Nevertheless, similar findings were observed when using preproGHRH-V5 cDNA construct in LoVo cells (not shown). As depicted in Fig. 8C, the 8.8 kDa intermediate form is not detected in LoVo cells, whereas transfection of the same construct in CHO cells containing furin did produce the 8.8 kDa intermediate form. Taken together, these results strongly support a primary role for furin in the first stepwise processing of proGHRH at the preproGHRH29-30 site.

In addition to LoVo cells, we also acquired CHO furin knockout cells (CHO FD11) and used them to further support the role of furin in the initial processing of proGHRH. CHOK1 (wild type) and CHO FD11 cells were both transfected with preproGHRH-GFP and then cell content and media were extracted and analyzed using Western blotting (Fig. 8D). In the FD11 cells, the 8.8 kDa was present, but

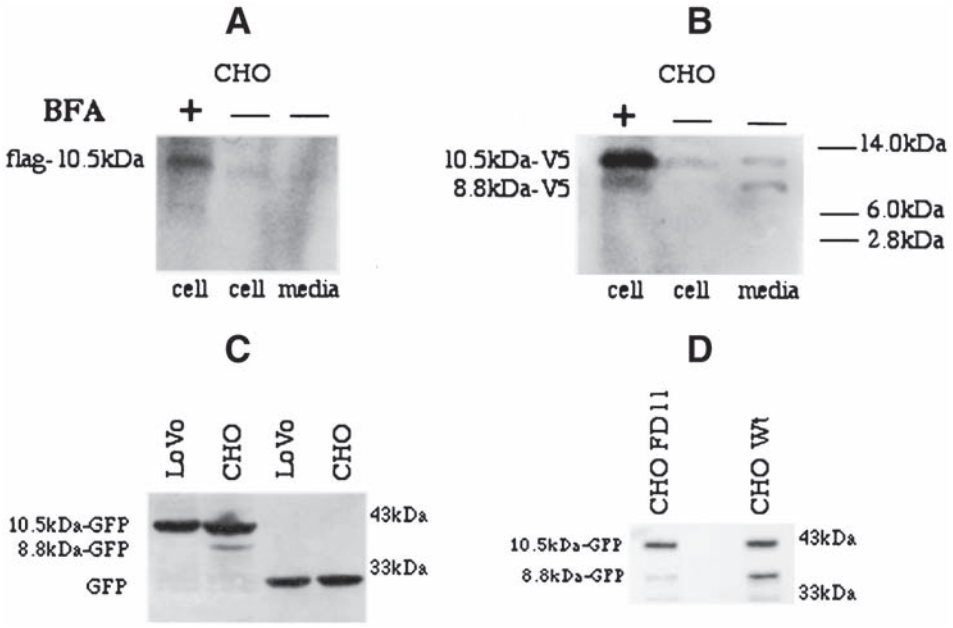

Fig. 8. Processing of the proFlagGHRH, proGHRH-V5, and proGHRH-GFP fusion proteins in CHO and LoVo cells treated with BFA. The extracted proGHRH-derived peptides from CHO cells transfected with the proFlag and proGHRH-V5 were visualized by Western blot analysis using anti-V5 and anti-flag antibodies. Some CHO cell groups were treated with 10 µg/mL BFA for 2 h (Panels A and B). Panel C shows a comparative processing of proGHRH in transfected LoVo and CHO cells with preproGHRH-GFP cDNA and visualized using anti-GFP antibodies. The two rows on the right show the GPG protein in cells transfected only with GFP cDNA. Panel D shows a comparative processing of proGHRH in transfected CHO K1 and CHO FD11 cells with preproGHRH-GFP cDNA and visualized using anti-GFP antibodies.

substantially reduced (approx threefold) in comparison to the same band in the CHO wild-type cells and no visible band was observed in the media (not shown).

Colocalization of PC1 with proGHRH in Primary Cultures of Hypothalamic Neurons

To further corroborate the role of PC1 on the processing of proGHRH, we determined the colocalization of proGHRH with PC1 in rat hypothalamic neurons. To this purpose, we used primary cultures of dissociated rat diencephalic neurons, commonly used in our laboratory, expressing high levels of PC1 and very low levels (as expected) of proGHRH *(4,29)*. Double-label ICC with antibodies directed against either GHRH peptide or PC1 reveal that a substantial proportion of these neurons express PC1 as shown before *(29)*, whereas the level of GHRH staining ranges between 2% and 4% as judge by counting more than 100 fields. Figure 9A shows a cell stained with anti-GHRH distributed in the cell body and processes (red fluorescence), and Fig. 9B shows a great number of cells stained with PC1 (green fluorescence). Panel 9C shows the colocalization of PC1 and GHRH.

Discussion

In 1999 we proposed for the first time a model of posttranslational processing for the GHRH precursor and suggested that more than one potentially biological peptide may result from this process *(4)*. After cloning the corresponding cDNAs, it was determined that the GHRH sequence is derived from the preproGHRH$_{1–104}$ precursor after removal of the signal leader sequence peptide, followed by two proteolytic cleavages, one at the N- and the other at the C-terminal regions of preproGHRH$_{30–74}$. This reaction generates a biologically active GHRH (preproGHRH$_{31–73}$) after the removal of the basic residues *(30,31)*. Our pulse-chase experiments provided substantial support for this hypothesis and further demonstrated the order by which the intermediate end products of processing are generated. These studies also suggested that more than 50% of the original precursor is processed within 30 min after its biosynthesis to give rise to an 8.8 kDa intermediate form followed by the formation of GHRH and GHRH-RP *(4)*. We also proposed that the 8.8 kDa form detected in the first stages of processing is derived from an N-terminal initial cleavage at the Arg^{29}-Arg^{30} of the original preproGHRH precursor. A remaining N-terminal preproGHRH$_{20–30}$ peptide of about 1.1 kDa may also be formed after the generation of the 8.8 kDa intermediate. However, the proteolytic enzymes involved in this process were unknown. Therefore, the primary objective of the current study was to determine which proconverting enzymes are involved in this process.

Utilizing radiolabeling protocols, three secretory cell lines were used in the investigation of the posttranslational

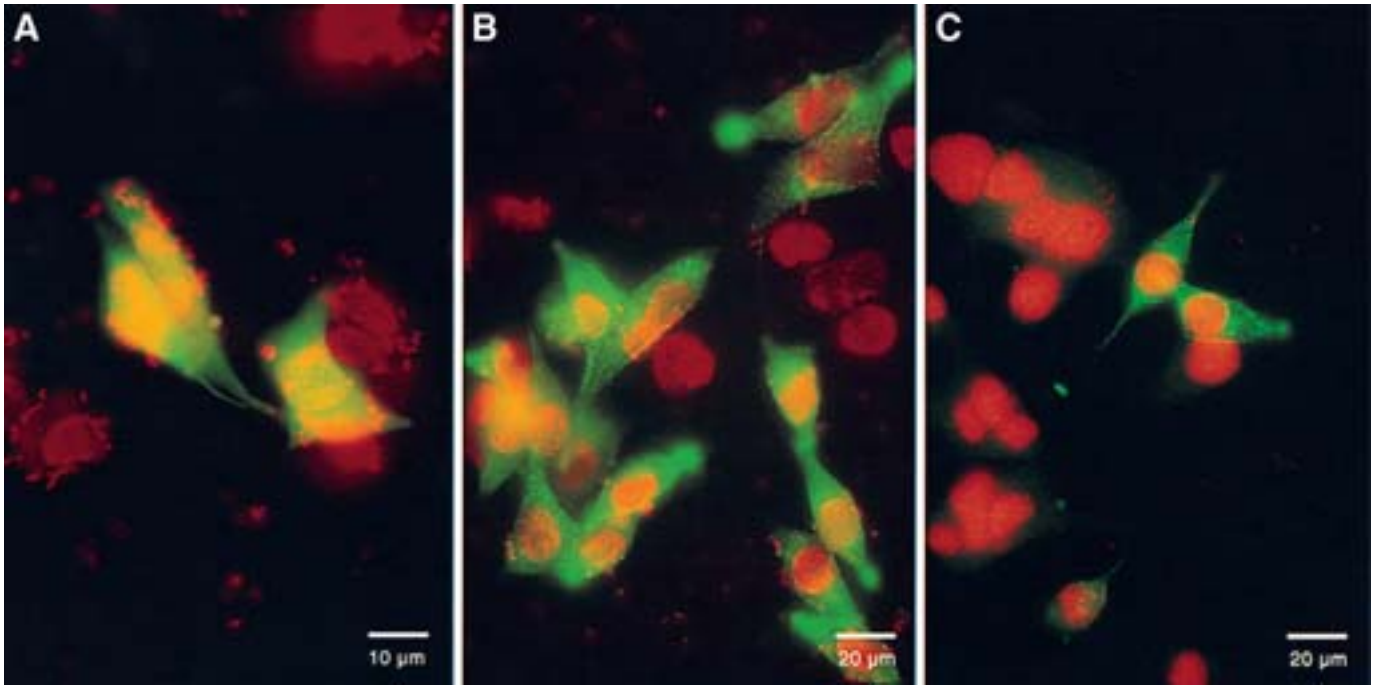

Fig. 7. Visualization of the fusion protein proGHRH-GFP and immunocytochemistry of translated wild-type preproGHRH cDNA in AtT-20 cells. AtT-20 cells cultured in four-chamber labTeck slides were fixed with 4% paraformaldehyde followed by immunoreaction with anti-GHRH or visualized by the translation of the GFP protein fused to proGHRH. Fluorescein isothiocyanate conjugated to goat anti-rabbit globulin was used as a probe. Panel A shows a diffuse cytoplasmic fluorescence in cells transfected with GPF alone. Panel B shows positive fluorescence in SGs in cells transfected with preproGHRH-GFP, and Panel C shows positive immunofluorescence in SGs of cells transfected with wild-type preproGHRH cDNA. Thirty millimeter slides were digitized with a video camera and appropriate macro lens using BioVisionframe Grabbera software (Perceptics Corporation, Knoxville, TN). The resulting images were printed with a Mitsubishi CP210 dye sublimation printer (Apunix Computer Services, San Diego, CA).

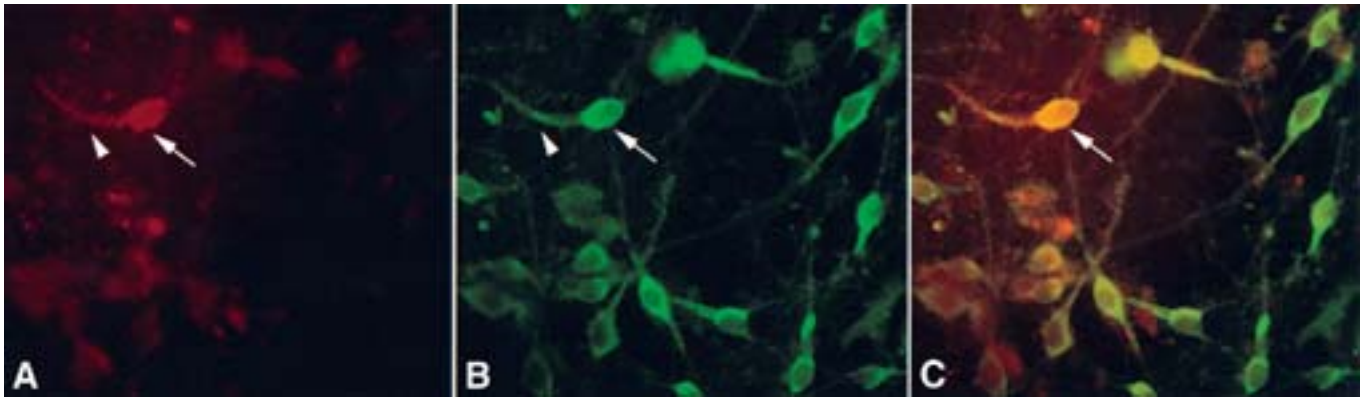

Fig. 9. Colocalization of PC1 with proGHRH in primary cultures of hypothalamic. Neuronal cells cultured for up to 14 d in four-chamber labTeck slides were fixed with 4% paraformaldehyde followed by immunoreaction with anti-PC1. Fluorescein isothiocyanate conjugated to goat anti-rabbit globulin was used as a probe. Texas Red-X-succimidylester directly conjugated to anti-GHRH antibodies was used as a probe for proTRH. Panel A shows positive immunostaining for proGHRH peptides (red color, arrows). Panel B shows positive immunostaining for PC1 (green color, arrow and arrowhead). Panel C shows the protein colocalization of proGHRH and PC1 (yellow-orange color indicated by arrows). Many neuronal cells (as expected) contain PC1 but not proGHRH (Panel B and C). Thirty millimeter slides were digitized with a video camera and appropiate macro lens using BioVisionframe Grabbera software (Perceptics Corporation, Knoxville, TN). Images of the red and green planes were combined using Adobe Systems, Mountain View, CA) to show areas of colocalization. The resulting images were printed with a Mitsubishi CP210 dye sublimation printer (Apunix Computer Services, San Diego, California).

modifications of proGHRH. AtT-20 cells, GH3 cells, and GH4-C1 cells proved useful in that they contain endogenous PC1, endogenous PC2, or neither endogenous PC1 nor PC2, respectively. These cell lines were transfected with preproGHRH in a variety of ways that manipulated these innate attributes. Many insights have been gained as to the role of PC1 and PC2 in the endoproteolytic cleavage of the immature proGHRH polypeptide into its mature form. The independent and codependent cleavage by the aforementioned enzymes was alluded to by the use of two antibodies, anti-GHRH and anti-GHRH-RP. These enzymes each display a unique recognition sequence site that aided in the positive identification of the degradated proGHRH protein fragments present. By regarding all pieces of evidence from these experiments and those by transfections in secretory and constitutive cells lines followed by Western blot analysis as a unit, and colocalization of PC1 with proGHRH in hypothalamic neurons, a nearly complete understanding of the posttranslational processing of proGHRH by furin, PC1, and PC2 has been established.

From our previous studies *(4)* we showed that the antibody anti-GHRH-RP recognizes the GHRH-RP segment of the proGHRH molecule. Our previously proposed model (Fig. 1) states that this segment is located from amino acid 75 to amino acid 104 on the proGHRH molecule. If this model is correct, the molecules of sizes 10.5 kDa, 8.8 kDa, and 3.6 kDa would contain GHRH-RP and, consequently, would be recognized by anti-GHRH-RP. Similarly, anti-GHRH was able to recognize all the extended forms of GHRH, the 10.5 kDa, 8.8 kDa, and 5.2 kDa GHRH (preproGHRH$_{31–74}$) peptides. Figures 3–5 show the processing of proGHRH in cell lines later immunoprecipitated using anti-GHRH and anti-GHRH-RP. Transfection solely with preproGHRH cDNA consistently produced two major peaks of 10.5 kDa and 8.8 kDa MM in the three cell lines analyzed with the exception of AtT-20 cells. The transfection of AtT-20 cells with preproGHRH resulted in a formation of GHRH and GHRH-RP. This indicates that PC1 has the ability to cleave proGHRH between amino acids 74 and 75. Comparing these results to GH3 cells, which contain endogenous PC2, transfected preproGHRH cDNA generated the GHRH precursor and the 8.8 kDa intermediate peptide. The presence of the 10.5 kDa and 8.8 kDa peptides agree with the profile elicited also by the GH4-C1 cells transfected with preproGHRH. These results clearly indicate that the generation of the 8.8 kDa intermediate peptide is independent of PC1. The most important observation in this set of studies was that the GH3 cells, which contain high endogenous levels of PC2 and furin, were able to generate significant GHRH and GHRH-RP only after transfection with PC1 cDNA.

GH4C1 cells transfected with preproGHRH gave rise to two peptide moieties, 10.5 kDa and 8.8 kDa, and with PC1 cDNA transfection, GHRH and GHRH-RP. This evidence exposes PC1's ability to cleave proGHRH between amino acids 74 and 75. The profiles given by the gel-slicing technique represents a snapshot of all the peptides containing the antibody recognition sequence in the cells. The low level of the 10.5 kDa peptide with respect to the 8.8 kDa and 5.2/3.6 kDa peptides suggests that PC1 cleaves early in the regulated secretory pathway, hindering the build up of the 10.5 kDa peptide. This observation is in agreement with the early maturation of PC1. A similar profile is observed when comparing the results of the preproGHRH and PC1 transfected GH4-C1 cells to preproGHRH transfected AtT-20 cells, which contain endogenous PC1. As in the GH3 cells, a sharp contrast exists between the levels of endogenous PC1 in AtT-20 cells, levels of transfected PC1 in GH4-C1 cells and the overall amount of processing by the respective cells lines. Further support to the radiolabeling studies came from transfection experiments of the fusion proteins proGHRH-GFP and proGHRH-V5 in AtT-20, GH3, and GH4C1 cells followed by Western blot analysis. The two fusion constructs used in all three cell lines produced the 10.5 kDa and 8.8 kDa peptides, but only AtT-20 produced the GHRH peptide. With proGHRH-GFP in GH3 cells, a weak band corresponding to the GHRH peptide was observed indicating that some activity of PC2 is present in the generation of GHRH and GHRH-RP peptides. Further support for the role of PC1 on the processing of proGHRH was determined by the colocalization of proGHRH with PC1 in primary cultures of hypothalamic neurons, an endogenous source of PC1 and proGHRH.

The use of constitutive cell lines with and without endogenous furin has been instrumental in determining the role of this enzyme in the cleavage of proGHRH at the R-R (29-30) residues. We used three fusion proteins to explore this question, proGHRH-GFP, proGHRH-V5, and FlagproGHRH. The latter, where the tag is at the amino terminal side of proGHRH specifically located between the signal peptide and proGHRH, as expected from our original hypothesis, showed no band in any of the secretory and constitutive cell lines. This supports the premise that furin produces a proteolytic cleavage at preFlagproGHRH$_{29–30}$ to generate a small peptide of about 1.8 kDa MM [made of a 1.1 kDa peptide *(4)* attached to Flag (approx 0.8 kDa)]. We analyzed the translation products derived from preFlagproGHRH cDNA transfection in AtT-20, GH3, GH4C1, CHO, and LoVo cells. The approx 0.8 kDa peptide is generally very difficult to detect by Western blot analysis. However, the possibility exists that after this initial cleavage the peptide was degraded or released in a constitutive fashion, but no band was detected in the release media of these transfections. The first evidence supporting a potential role for furin was demonstrated when we used the CHO constitutive cell line (containing furin, but no PC1 or PC2) transfected with preFlag-proGHRH cDNA and subjected to BFA treatment. However, this cell line contains other convertases

including PACE4, PC5, and PC7 that could be also responsible for such a cleavage. However, the experimental data presented in this study support the role of furin in the initial processing cleavage of proGHRH. Similarly, translation products of the proGHRH-V5 construct transfected into CHO cells and treated with BFA showed, as expected, more accumulation of the GHRH precursor and a second weaker band corresponding to the 8.8 kDa peptide. BFA treatment disassembles the Golgi, and these results show that this organelle is the likely location of the first processing step of proGHRH maturation.

The first conclusive evidence implicating furin in the processing of proGHRH at the 29-30 amino acid residues came from the transfection of preproGHRH-GFP cDNA in LoVo (no furin) and CHO (furin) cells. The most remarkable result was that LoVo cells were unable to process proGHRH at all, whereas CHO cells generated, as expected, the 8.8 kDa intermediate by the action of furin. CHO FD11 furin knockout cells also supported this finding. Although, in much lesser degree, the 8.8 kDa band was produced in CHO FD11 cells transfected with preproGHRH-GFP, it was reduced approx threefold in comparison to CHO wild-type cells transfected with the same cDNA. In conclusion, the formation of the 8.8 kDa peptide alludes to the action of furin early in the secretory pathway, which has the ability to cleave proGHRH between amino acids 29 and 30. However, this enzyme does not appear to be a dominant player in the enzymatic digestion of the 8.8 kDa peptide.

Our results verify the hypothesis that the 8.8 kDa intermediate form is primarily cleaved by PC1. The more elusive question is where each enzyme preferentially cleaves the polypeptide. The distribution of furin and PC1 in both endocrine and neuroendocrine systems further demands an understanding of when each of these enzymes matures and thus can efficiently cleave the precursor peptide to its active form. PC1 has been found to undergo autocatalytic cleavage and consequently matures early in the regulated secretory pathway. Zymogen processing of PC1 is established within a few minutes from the initiation of its precursor's synthesis *(32)*, but the pro-segment remains attached to PC1 effectively inhibiting the enzyme, which then gets activated through a secondary pro-segment cleavage when it reaches the TGN and/or immature secretory granules. The same applies to furin *(33)*. The model proposed here describes the initial cleavage site to be between amino acids 29 and 30. This proteolytic cleavage converts the 10.5 kDa polypeptide into two fragments: a smaller peptide with unknown function and a larger 8.8 kDa peptide containing both the GHRH and GHRH-RP entities. This hypothesis finds much support in the experiments mentioned above. Our results also show that this processing occurred in an orderly fashion where processing of the 8.8 kDa form by PC1 is furin-dependent. It could be possible that after the initial cleavage by furin the 8.8 kDa peptide changed its protein conformation to allow the access of PC1 to its cleavage substrate.

Unlike PC1, PC2 matures slowly and with the aid of a neuroendocrine secretory protein, 7B2, which facilitates the intracellular transport and activation of PC2 *(34,35)*. Requirements for activation, such as a low pH and a high concentration of calcium for full activity, inhibit PC2 from fully maturing until late in the secretory pathway. PC2's requirements are consistent only with the intracellular environment found in the late secretory pathway. This suggests that PC2 is unable to alter the structure of proGHRH early in the pathway and consequently may not process proGHRH when it is present in the 8.8 kDa and smaller forms. The interesting point to note is that, although these are the favored modifications of PC1 or PC2, they both cleave in the same manner and thus can assume the other enzyme's duties in its absence. PC1 and PC2 both cleave with the general motif (Arg/Lys)-$(X)_n$-Arg, where n = 0, 2, 4, or 6 and X is any amino acid except cystine and rarely proline. Similar cleavage specificities can result in a certain amount of redundancy between the convertases in some cases and not in others. In the case of proGHRH it seems that while PC2 can effect some GHRH production, PC1 is much more efficient in performing this cleavage. The reason may be related to the presence of a positively charged His at the P1' (at the acidic pH of the granules) of the monobasic cleavage site **R**S**R**FN**R**^{74}↓HL of proGHRH.

It is important to note that we have previously shown that some GHRH and GHRH-RP may be release via the constitutive pathway in primary cultures of hypothalamic neurons *(4)*. This is consistent with the hypothesis of an early processing in the trans Golgi network. Indeed our results indicate a direct involvement of furin and PC1 in the processing of proGHRH. Taken together this may suggest that most of the processing of proGHRH may occur early in the secretory pathway at the level of the trans Golgi network or immature secretory granules. In summary, the data presented in this work support the hypothesis that proGHRH is initially cleaved by furin at preproGHRH$_{29–30}$ at the TGN level, followed by at least an initial second processing step in the same compartment by PC1 at preproGHRH$_{74}$ to generate GHRH and GHRH-RP peptides, respectively. Further processing in the SGs may occur by the action of PC1 or PC2. Based on the previous *(4)* and current study, Fig. 10 depicts the propose model of stepwise processing of proGHRH during its traffic through the secretory pathway. In a recent study *(36)* where PC1 knockout mice were generated, it was reported that mice lacking PC1 are normal at birth, but fail to grow normally and are about 60% of normal size at 10 wk. They lack mature GHRH, have low pituitary growth hormone (GH), and hepatic insulin-like growth factor-1 mRNA levels and resemble phenotypically the "little" mouse. These in vivo findings further support our hypothesis and prove the relevance of PC1 as

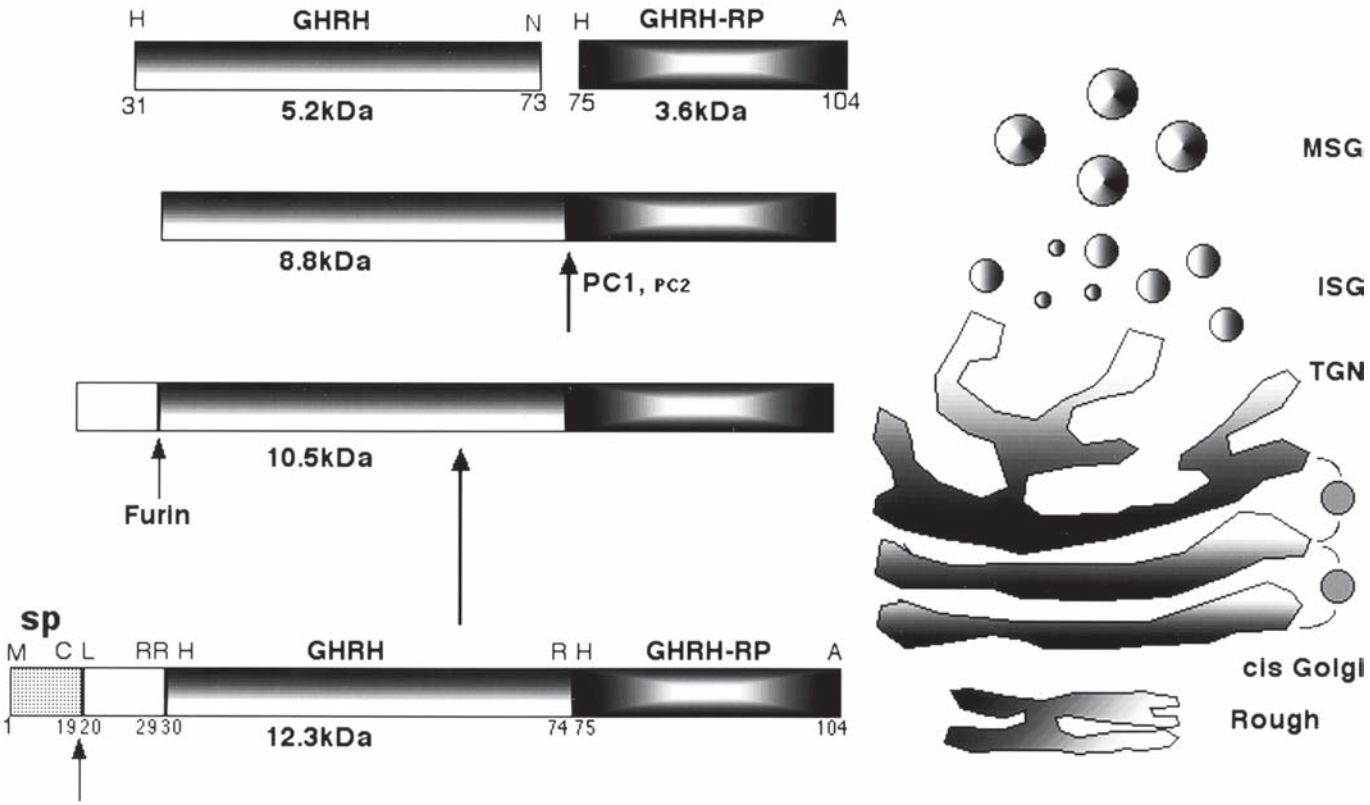

Fig. 10. Proposed stepwise of model of processing of proGHRH within the regulated secretory pathway.

a key neuroendocrine convertase regulating the processing of proGHRH.

Materials and Methods

RNA Isolations

Total RNA was isolated from cultured cells at 80% confluence using TRIzol® Reagent according to the supplier's recommended method (Invitrogen). RNA quality was accessed by UV-absorbance and formaldehyde denaturing gel electrophoresis.

cDNA Constructs

Rat preproGHRH cDNA was amplified from fetal hypothalamic neuronal cell RNA using transcript specific primers and RT-PCR. The upstream primer also positioned a kozak concensus sequence (GCCACCATG) at the 5' terminus of the cDNA, while the downstream primer provided a stop codon (TGA) at the 3' terminus. This cDNA was A/T cloned into pCR®II-TOPO (Invitrogen) and a *Pst* I/*BamH* I fragment containing the rat preproGHRH was isolated and subcloned into the mammalian cell expression vector pcDNA3.1/Zeo+ (Invitrogen). Sequence frame and fidelity were verified by primer-mediated cycle sequencing reactions and analysis on an Applied Biosystems 377 DNA Sequencer. PC1 and PC2 constructs were made by inserting a full-length mouse cDNA for either PC1 or PC2 into the *Hind*III blunt restriction sites of the expression vector Rc/CMV (Invitrogen). Pre-Flag-proGHRH and preproGHRH-V5 constructs were generated by PCR mutagenesis as was recently done for β-secretase BACE *(37)* and SKI-1 *(38)*. To create the preproGHRH-GFP construct, preproGHRH was subcloned into apEGFP-NI in frame to place a GFP tag at the C-terminus of the translated proGHRH molecule.

Antibodies

Anti-GHRH and anti-GHRH-RP were made to recognize the entire GHRH and GHRH-RP sequence, respectively. These antibodies were kindly provided by Dr. Ora Pescovitz from Indiana University and fully characterized in our previous publication *(4)*.

Tissue Culture for Cell Lines

All the cell lines used in this study were plated in 75-cm^2 maintenance flasks (Corning Costar Corporation) at a density of 10–20 × 10^6 cells per flask, and for transfection experiments in 100 mm Petri dishes at a density of 10 × 10^6 cells. They were grown at 37°C in 5% CO_2 in an air atmosphere at 90% humidity. AtT-20 cells were grown in Dulbecco's modified Eagle's medium (DMEM Life Technologies, Inc., Gaithersburg, MD): 10% fetal calf serum, 25 μg/μL penicillin, and 25 μg/μL streptomycin. GH3 cells were

grown F12K medium (Life Technologies, Inc., Gaithersburg, MD) containing 7% of horse serum and 3% of fetal calf serum, 1.25 mL penicillin, 1.25 mL streptomycin, and 0.75 g $NaHCO_3$. GH4C1 cells were grown in Hams F10 medium (Life Technologies, Inc., Gaithersburg, MD) containing containing 7% of horse serum and 3% of fetal calf serum, 2.5 mL penicillin, and 2.5 mL streptomycin. The LoVo Cells were grown for 6 d in Ham's F-12k media containing 10% fetal calf serum, 25 μg/μL penicillin, and 25 μg/μL streptomycin. The CHO cells were grown for 6 d in Ham's F-10 media containing 10% fetal calf serum, 25 μg/μL penicillin, and 25 μg/μL streptomycin. CHO K1 cells were a wild-type CHO cell line. CHO FD11 cells were a cell line irradiated to remove furin activity. CHO FD11 furin+ cells were a stable pool of CHO FD11 cells transfected with furin cDNA. CHO FD11 furin+ cells were grown in the media described above, with an additional 200 μg/mL and 400 μg/mL of geneticin, respectively. The CHO mutant cell lines were acquired from our collaborator Dr. Nabil Seidah.

Primary Cultures of Hypothalamic Neurons

Hypothalamic neuronal cultures were produced as previously described *(29)*. In brief, timed pregnant female rats on d 17 of gestation were anesthetized with pentobarbital (60 mg/kg), the abdominal cavity was opened, and the fetuses were removed. Each fetus was decapitated and the diencephalon was isolated. Diencephalic tissue was dissociated to single cells by neutral protease digestion (1 unit/tissue, Sigma, MO). The cells were cultured for up to 14 d in L-15-Dulbecco's modified Eagle's medium (D-MEM/L-15) containing 10% fetal calf serum (FCS; Gibco BRL, MD) and supplemented with various additives *(29)*. Prior to plating, all wells were coated with poly-D-lysine (20 μg/mL, Sigma). For immunocytochemistry (ICC), the cells were plated on four-chamber glass LabTek (Nunc Inc., Naperville, IL) slides (10^6 cells/mL).

Transient Transfection of Cells

The cells were split 2 d prior to transfection for AtT-20 cells and 3 d before transfection for GH3, GH4-C1, LoVo, and CHO cells. This was to ensure that there are at least 20–30 million cells present in each plate. The transfection was carried out using the Lipofectamine Plus system (Life Technologies, Inc.). In a sterile 15 mL conical tube, 4 μg of the particular preproGHRH cDNA (1 μg/μL) was added to 20 μL PLUS reagent and 750 μL serum-free medium and incubated for 15 min. Depending on the cell line, preproGHRH cDNA was transfected alone or in combination with PC1 cDNA (1 μg/μL) and/or PC2 cDNA (1 μg/μL). The efficiency of the transfection when not included in the plasmid was checked by the addition of 2 μg of GFP cDNA in combination with the aforementioned cDNA. The serum-free medium described above was particular to each cell line (the AtT-20 cells receive DMEM serum-free medium, GH3 cells received F12K serum-free medium, and the GH4-C1 cells received Ham's F10 serum-free medium) and identical to the media discussed above except for the lack of horse serum and fetal calf serum. After the 15 min incubation period, 30 μL Lipofectamine and 750 mL serum-free media were added to the conical tube and incubated for another 15 min. During this time, the Petri dish was washed with 10 mL serum-free medium. This medium was aspirated after the 15 min incubation period and 5 mL serum-free medium was added in addition to 1.5 mL of the transfection solution. The cells were then incubated for 3 h. Following the 3 h, 5 mL of medium with double the concentration of serum and antibiotics was added to the Petri dish to obtain normal concentration of both serum and antibiotics. The medium was replaced 18 h later with normal medium and 300 μL of sodium butyrate was added to the cells 17 h prior to radiolabelling.

Radiolabeling AtT-20, GH3, and GH4-C1 Cells

AtT-20, GH3, and GH4-C1 cells were transfected preproGHRH cDNA as described above. Untransfected cells were also radiolabeled and used as a control. Leucine-, tryptophan-, and valine-free media were made up for each cell line. The medium was combined with normal medium at a 9:1 ratio for AtT-20 cells and GH3 cells and a 9:2 ratio for GH4-C1 cells. The Petri dishes were aspirated and 4 mL of the 9:1 or 9:2 medium was added. Each dish then received 60 μL tryptophan, 60 μL valine, and 100 μL [3-4-5-^{3}H]leucine (156 Ci/mol) (NEN, Boston, MA). The plates were incubated for 4 h and then harvested for immunoprecipitation *(4)*.

Extraction and Immunoprecipitation

After radiolabeling the cells were gently harvested with 5 mL of cold PBS and centrifuged for 5 min at 170*g*. After removing the PBS, 300 μL of 2 *N* acetic acid containing Inhibitor Cocktail (Sigma) was added to the pellet. The samples were then boiled for 10 min and microcentrifuged at 16,000*g* for 10 min. After centrifugation, the lysate was transferred to a new Eppendorf tube and centrifuged again. If a pellet formed, the procedure was repeated until a clear lysate was produced. The lysate was freezed dried until use. The dried samples were resuspended with 200 μL of 100 m*M* phosphate buffer, pH 7.4. The 100 m*M* phosphate buffer was made by combining 47.5 mL of solution A (6.9 g NaH_2PO_4 brought to 250 mL with ddH_2O), 202.5 mL solution B (13.4 g Na_2HPO_4 brought to 250 mL with ddH_2O), and 2.5 g BSA. This is brought to 500 mL with ddH_2O.

Antibody-conjugated sepharose beads were used for this procedure. Preparation consisted of combining 15 μL of 50% protein A-sepharose bead slurry, 0.5 mL ice-cold PBS, and 1 μL of antibody in a 1.5 mL conical microcentrifuge tube. The suspensions were mixed thoroughly and placed on the tumble rotator at 4°C in a walk-in refrigerator overnight. The beads were then washed. The suspension was then

microcentrifuged for 2 s at 16,000*g*, 4°C. The supernatant was aspirated and 1 mL nondenaturing lysis buffer (5 mL Triton X-100, 25 mL of 1 *M* Tris pH 7.4, 75 mL of 1 *M* NaCl, 5 mL of 0.5 *M* EDTA, 2 mL of 5% NaN_3 was brought to 489.3 mL with ddH_2O) was added to resuspend the beads. The beads were mixed by inversion of the tube three or four times. The wash was repeated three times. During the final wash nondenaturing lysis buffer was not added, but the beads were washed with PBS. The sample was microcentrifuged and then aspirated. The sample was finally boiled for 10 min, the supernatant gathered and resuspended with 30 µL 1X sample buffer for use with SDS-PAGE.

SDS-PAGE

Radiolabeled and immunoprecipitated samples were loaded onto a 1.5 mm SDS tricine polyacrylamide gel using Protean 16 cm cell apparatus (Bio-Rad Laboratories, Hercules, CA). Following electrophoresis, the gels were sliced into 2.2 mm slices using a gel slicer (Hoeffer Scientific Instruments, San Francisco, CA) and placed in 10 mL scintillation vials. Peptides were extracted using 0.5 mL 2 *N* acetic acid. The vials were placed at 4°C for 3 d before counting. Samples were then immersed in 5 mL scintillation fluid (Bio Safe II, RPI, Mount Prospect, IL) and the radioactivity was counted using a scintillation counter.

Western Blot Analysis

Forty-eight hours after transfection BFA-treated and -nontreated cells were washed with PBS and peptides were acid extracted as described above. Fifty micrograms of total protein was applied to Tricine-SDS-PAGE gels. Following electrophoresis, proteins were electroblotted onto Immobilon P^{sq} membranes (Millipore, Bedford, MA) or Immobilon P membranes for GFP tagged proteins for immunodetection. The membranes were probed overnight at 4°C with a 1/1000 dilution of either anti-GFP, 1/2000 dilution of anti-V5 (Invitrogen, Carlsband, CA), and 1/2000 dilution of anti-Flag (Stratgene, La Jolla, CA) antibodies. An alkaline phosphatase-linked goat anti-rabbit immunoglobulin secondary antibody (1:2000 final dilution) or goat anti-mouse immunoglobulin was used and immunoreactive bands visualized by Immunolite Assay as described by the manufacturer (Bio-Rad Laboratories, Richmond, CA).

Immunocytochemistry (ICC)

Hypothalamic neurons (3×10^5) from 12 d old cultures and AtT-20 cells commonly grown in our laboratory were fixed with 4% paraformaldehyde in PBS and subjected to an immunocytochemistry protocol as previously described *(15,29)*. Immunoreaction of the primary anti-PC1 antibody with the hypothalamic neurons was performed at 4°C for 24 h. Goat anti-rabbit immunoglobulin conjugated with fluorescein isothiocyanate (FITC) was used as the fluorescence marker. We previously established the conditions for immunodetection of PC1 in primary neurons *(15)*. The optimal dilutions were found to be 1:1000 for the primary antibody and 1:2000 for the secondary antibody with an incubation time of 24 h at 4°C for the primary antibody and 2 h at room temperature for the secondary antibody. For colocalization experiments, cells previously stained with anti-PC1 followed with FITC probe (green color) were then incubated with anti-GHRH-Texas Red for 24 h at 4°C. We have previously described the conjugation conditions of Texas Red (red color) to different antibodies, as well as their ability to obtain successful colocalization with other proteins, in experiments demonstrating the colocalization of proTRH with the PC1 *(15)*, and proTRH with carboxyl peptidase E and D *(39)*. Control experiments, including the incubation of cells without primary antibody or with preimmune sera, and blocking of the primary antibody with the synthetic peptide for which the antibody were generated, were performed and did not show significant positive staining.

Reverse Transcription-PCR of AtT-20, GH3, and GH4-C1 RNAs

Total RNA (3.7 µg) isolated from AtT-20, GH3, or GH4-C1 cultured cells was DNAse treated and random hexamer primed cDNA was synthesized with or without reverse transcriptase. Sequence specific primers were used in separate 50 µL PCR amplifications containing 500 ng cDNA. Reactions were cycled 23 times for amplification of PC1 or PC2 and 20 times for GAPDH. A 10 µL sample of each reaction was run on a 3% agarose gel (TAE) containing ethidium bromide. A fluorescing image of the gel was captured using a BioRad Gel Doc 2000 digitizer. The following primer pairs were used for PC1, PC2, and GAPDH amplifications:

PC1 upstream
5'- GATCCAATGTGGAATCAGCAGTGG-3'
PC1 downstream
5'- GCCATCCAGCATTCTTATGCCTCC-3'
PC2 upstream
5'- GAGTCCGAAAGCTCCCCTTTGCAG-3'
PC2 downstream
5'- GAACCAGTCATCTGTGTATCGAGG-3'
GAPDH upstream
5'- ACCACAGTCCATGCCATCAC-3'
GAPDH downstream
5'- TCCACCACCCTGTTGCTGTA-3'

Acknowledgments

We wish to thank Dr. Ora H. Pescovitz from Indiana University for providing the anti-GHRH and anti-GHRHRP antibodies. We would also like to thank Ms. Virginia Hovanesian for her imaging work in the immunocytochemistry studies. These studies were supported in part by NIDDK/NIH grant DK58148 to EAN.

References

1 Steiner, D. F. (1998). *Curr. Opinion Chem. Biol.* **2,** 31–39.
2 Seidah, N. G. and Chretien, M. (1999). *Brain Res.* **848,** 45–62.
3 Arvan, P. and Castle, D. (1998). *Biochem. J.* **332,** 593–610.
4 Nillni, E. A., Steinmetz, R., and Pescovitz, O. H. (1999). *Endocrinol.* **140,** 5817–5827.
5 Seidah, N. G., Chretien, M., and Day, R. (1994). *Biochimie* **76,** 197–209.
6 Guillemin, R., Brazeau, P., Bohlen, P., Esch, F., Ling, N., and Wehrenberg, W. B. (1982). *Science* **218,** 585–587.
7 Rivier, J., Spiess, J., Thorner, M., and Vale, W. (1982). *Nature* **300,** 276–278.
8. Hofman, P. L. and Pescovitz, O. H. (1998). In: *The cellular basis of pediatric endocrinology.* Handwerger, S. (ed.), Humana Press: Totowa, NJ.
9. Loh, Y. P., Beinfeld, M. C., and Birch, N. P. (1993). In: *Mechanisms of intracellular trafficking and processing proproteins.* Loh, Y. P. (ed.), CRC Press: Boca Raton, FL, pp. 179–224.
10. Mains, R. E., Dickerson, I. M., May, V., et al. (1990). *Front. Neuroendocrinol.* **11,** 52–89.
11 Seidah, N., Marcinkiewicz, M., Benjannet, S., et al. (1991). *Mol. Endocrinol.* **5,** 111–122.
12. Seidah, N. G., Gaspar, L., Mion, P., Marcinkiewicz, M., Mbikay, M., and Chretien, M. (1990). *DNA* **9,** 415–424.
13 Lusson, J., Vieau, D., Hamelin, J., Day, R., Chretien, M., and Seidah, N. G. (1993). *Proc. Natl. Acad. Sci. USA* **90,** 6691–6695.
14 Schafer, M.-H., Day, R., Cullinan, W. E., Chretien, M., Seidah, N., and Watson, S. (1993). *J. Neurosci.* **13,** 1258–1279.
15 Schaner, P., Todd, R. B., Seidah, N. G., and Nillni, E. A. (1997). *J. Biol. Chem.* **272,** 19958–19968.
16 Pu, L. P., Ma, W., Barker, J., and Loh, Y. P. (1996). *Endocrinol.* **137,** 1233–1241.
17 Nillni, E. A., Friedman, T. C., Todd, R. B., Birch, N. P., Loh, Y. P., and Jackson, I. M. D. (1995). *J. Neurochem.* **65,** 2462–2472.
18 Friedman, T. C., Loh, Y. P., Huang, S. S., Jackson, I. M. D., and Nillni, E. A. (1995). *Endocrinol.* **136,** 4462–4472.
19 Steiner, D. F., Smeekens, S. P., Ohag, S., and Chan, S. J. (1992). *J. Biol. Chem.* **267,** 23435–23438.
20 Smeekens, S. P., Montag, A. G., Thomas, G., et al. (1992). *Proc. Natl. Acad. Sci. USA* **89,** 8822–8826.
21. Rouille, Y., Duguay, S. J., Lund, K., et al. (1995). *Front. Neuroendocrinol.* **16,** 332–361.
22 Brakch, N., Galanopoulou, A. S., Patel, Y. C., Boileau, G., and Seidah, N. G. (1995). *FEBS Lett.* **362,** 143–146.
23 Benjannet, S., Rondeau, N., Day, R., Chretien, M., and Seidah, N. G. (1991). *Proc. Natl. Acad. Sci. USA* **88,** 3564–3568.
24 Thomas, L., Leduc, R., Thorne, B. A., Smeekens, S. P., Steiner, D. F., and Thomas, G. (1991). *Proc. Natl. Acad. Sci. USA* **88,** 5297–5301.
25 Benjannet, S., Reudelhuber, T., Rondeau, N., Chretien, M., and Seidah, N. G. (1992). *J. Biol. Chem.* **267,** 11417–11423.
26 Breslin, M. B., Lindberg, I., Benjannet, S., Mathis, J. P., Lazure, C., and Seidah, N. G. (1993). *J. Biol. Chem.* **268,** 27084–27093.
27 Hoflehner, J., Eder, U., Laslop, A., Seidah, N. G., Fischer, R., and Winkler, H. (1995). *FEBS Lett.* **360,** 294–298.
28. Perez de la Cruz, I. and Nillni, E. A. (1996). *J. Biol. Chem.* **271,** 22736–22745.
29. Nillni, E. A., Luo, L. G., Jackson, I. M. D., and McMillan, P. (1996). *Endocrinol.* **137,** 5651–5661.
30. Mayo, K. E., Vale, W., Rivier, J., Rosenfeld, M. G., and Evans, R. M. (1983). *Nature* **306,** 86–88.
31. Mayo, K. E., Cerelli, G. M., Rosenfeld, M. G., and Evans, R. M. (1985). *Nature* **314,** 464–467.
32. Benjannet, S., Rondeau, N., Paquet, L., et al. (1993). *Biochem. J.* **294,** 735–743.
33. Anderson, E. D., Molloy, S. S., Jean, F., Fei, H., Shimamura, S., and Thomas, G. (2002). *J. Biol. Chem.* **277,** 12879–12890.
34. Muller, L., Zhu, X., and Lindberg, I. (1997). *J. Cell Biol.* **139,** 625–638.
35. Muller, L. and Lindberg, I. (1999). *Prog. Nucleic Acid Res. Mol. Biol.* **63,** 69–108.
36. Zhu, X., Zhou, A., Dey, A., et al. (2002). *Proc. Natl. Acad. Sci. USA* **99,** 10293–10298.
37. Elagoz, A., Benjannet, S., Mammarbassi, A., Wickham, L., and Seidah, N. G. (2002). *J. Biol. Chem.* **277,** 11265–11275.
38. Benjannet, S., Elagoz, A., Wickham, L., et al. (2001). *J. Biol. Chem.* **276,** 10879–10887.
39. Nillni, E. L., Xie, W., Mulcahy, L., Sanchez, V. C., and Wetsel, W. C. (2002). *J. Biol. Chem.* **277,** 48587–48595.